A genetic algorithm for identifying the single diode model parameters of a photovoltaic panel

J. D. Bastidas-Rodriguez[a], G. Petrone[b], C. A. Ramos-Paja[c], G. Spagnuolo[b]

[a]*Universidad Industrial de Santander, Escuela de Ingenierías Eléctrica, Electrónica y de Telecomunicaciones, Colombia*
[b]*University of Salerno, Dep. of Informatics, Electrical Eng. and Applied Mathematics-Italy*
[c]*Facultad de Minas, Universidad Nacional de Colombia - Sede Medellín, Colombia*

Abstract

In this paper the identification of the single-diode model of photovoltaic (PV) generators operating in outdoor conditions has been carried out. The non-linear equation system, describing the PV source in five operating points, is re-written as an optimization problem and it is solved by using a genetic algorithm. The parameters of the single-diode model are evaluated for different combinations of irradiance and temperature conditions. Contrary to several approaches proposed in literature such analysis shows that all the parameters need to be adjusted with respect the environmental conditions to reduce the errors in the current, power and energy predictions.

Keywords: Photovoltaic modeling, Parameters calculation, single diode model, Genetic algorithm

1. Introduction

Photovoltaic (PV) generators are highly non-linear systems and their behavior depends strongly on the environmental conditions.

The variations of irradiance and temperature along the day modifies the current vs. voltage (I-V) and power vs. voltage (P-V) characteristics of the PV modules; therefore, it is necessary to connect the PV module or array to a power converter that searches the operating point where the PV generator produces its maximum power, that is the Maximum Power Point (MPP).

Given the variability of the PV sources, it is important to have accurate and comprehensive models for PV modules as well as parameterization procedures to: evaluate the performance of the Maximum Power Point Tracking (MPPT) strategies, evaluate different PV array configurations, perform economic analysis of PV installations, estimate the amount of energy produced by a PV system, evaluate the impact of the PV system on the reliability of a transmission and distribution system [7], design further control strategies, or for diagnostic purposes.

The single-diode model, shown in Fig. 1, is widely adopted for modeling PV sources [1, 26, 22, 36, 10] and its five parameters I_{ph}, I_{sat}, η, R_s, R_h, which characterize the PV source for a specific environmental condition, can be calculated following different procedures available in literature. Some of them consider that all parameters varies with the irradiance and/or temperature [19, 10], while other procedures assumes that three parameters are constant and two parameters are functions of the irradiance and temperature [36, 24, 33, 28].

Methods, introduced in [1, 30, 8, 9], perform simplifications to obtain a system of non-linear equations, which is solved in the operating points provided by the manufacturer datasheet to obtain the parameters of the model. Other authors [2, 33, 28] use explicit equations to find some parameters (e.g. PV current, inverse saturation current and thermal voltage) and they use iterative methods to adjust the values of the remaining ones (e.g. series and parallel resistances) to fit the model with the information taken from the datasheet.

Other approaches use optimization techniques in order to estimate the values of the five parameters that fit the model in some reference points (i.e. experimental measurements or datasheet information) of a given I-V curve. Considering that the magnitudes of the five parameter are different (e.g. I_{sat} is in nA while I_{ph} is in A) and that the PV module is described by an implicit non-linear equation, the estimation of the single-diode model parameters is a complex non-linear ill-conditioned problem. Hence, in the last years different methods based on computational intelligence have been proposed to solve this problem, where the fitness function is, in most of the cases, the Root Mean

2

Squared Error between the model and the reference data.

The computational intelligence based methods use different algorithms to optimize the fitness function: Genetic Algorithms [17, 23], Particle Swarm [31], Generalized Reduced Gradient [24], Pattern Search [3], Differential Evolution [31], Artificial Bee Swarm [6], Bacterial Foraging [29], among others. The methods to estimate the PV module parameters differ not only for the optimization method, but also in the procedure to reproduce the I-V curves under different conditions, and the procedures used to reduce the convergence time. For instance, some methods calculate the parameters in a given irradiance and temperature conditions and then use translation equations to obtain the values of the parameters for different irradiances and temperatures [24, 31, 3, 32]. Other techniques propose to calculate the parameters for each operating condition [16, 38]. The definition of a limited search space helps to reduce the minimization time, that is why some authors define ranges for some [17, 23] or all [16, 13, 5] module parameters that contain the solution.

Despite the large amount of stochastic techniques available to calculate the parameters of a PV module, just few techniques propose to use a limited number of points of the reference I-V curve to perform the optimization procedure. In the studied techniques only [24] and [31] use the three main points of an I-V curve to estimate the module parameters. Those methods pose a system of five non-linear equations without any simplification to find the five parameters of the model. Although the errors obtained with both methods are small, they assume that the values of one ([31]) or three parameters ([24]) are constant for different irradiance and temperature conditions, and that some parameters depend on temperature (like I_{sat} and η) or irradiance (like R_h) only. Such an assumption could produce an error in the evaluation of a PV module productivity along the time because the degradation produced by the outdoor operation may modifies one or more parameters [25, 14, 34, 18, 20].

In order to show the dependencies of all parameters with respect to the environmental operating conditions, in this paper the five parameters of the single-diode model have been evaluated by reducing a system of six non-linear

equations in a single objective function. Thus, the solution is obtained by solving the optimization problem by using a Genetic Algorithm (GA). The objective function is constructed by using experimental I-V curves or, for many commercial PV panels, by means of the information available in the free database of "System Advisor Model" (SAM) provided by the U.S. Department of Energy. Moreover, the search ranges are defined with respect to the approximated values of the parameters of each module in order to obtain proper search ranges for each module, thus providing a good initial population to the GA. This is to reduce the convergence times and reduce the variability of the solutions (parameters) for a given irradiance and temperature condition.

The proposed method has some advantages with respect to other techniques proposed in literature, like [17, 23]. One of the advantages is the reduced calculation burden, since the proposed method uses only five points of the I-V curve and 20 individuals for the population, while [17, 23] use much more points of the I-V curve, a larger population size (30 individuals for [17]) and a complex method (hybrid GA) in [23]. Moreover, this paper shows in detail the selection and definition of the GA settings, which contrasts with [17, 23] where some of the GA settings are not justified or it is not clear how to implement them [17]. Furthermore, in GA the guess solution and the search range have to be chosen in a proper way in order to ensure a good performance: this paper is aimed at covering this issue, since in other papers [17, 23] the guess solution is not defined and the constraints are not justified in depth.

The paper is organized as follows: Section 2 presents the single-diode model of a PV module. Section 3 introduces the proposed method to calculate the five parameters of the model, and in Section 4 simulation results obtained by using the proposed method are shown. In Section 5 the analysis of the parameters variation for different irradiance and temperature conditions is presented. Finally, the Conclusions close the document.

4

2. Single-diode model of a PV module

Assuming uniform operating conditions, the model in Fig. 1 can be used for describing a single PV cell, a PV module or a PV array provided that the five parameters characterizing the PV model are calculated accordingly.

In the following the authors refer to a PV module made of N_s cells connected in series working in uniform irradiance and temperature conditions, this is because the PV manufacturer's datasheet report directly the I-V curves and P-V curves of the PV panel in STC, i.e. uniform conditions.

By using simple calculations, the corresponding analytical equation (1) is obtained:

$$I = I_{ph} - I_{sat} \cdot \left(\exp \left(\frac{V + R_s \cdot I}{\eta \cdot V_t} \right) - 1 \right) - \frac{V + R_s \cdot I}{R_h} \tag{1}$$

where I and V are the current and the voltage of the PV source, respectively, I_{ph} is the current produced by the photovoltaic effect, I_{sat} is the inverse saturation current of the diode, η is the ideality factor of the P-N junction, R_s and R_h are the series and parallel resistances, respectively. $V_t = N_s \cdot k \cdot T / q$, where k is the Boltzmann constant, q is the electron charge, and T is the cell temperature in Kelvin degrees.
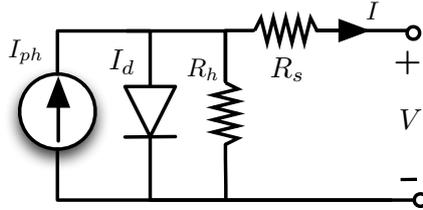

Figure 1: Single-diode model of a PV source operating in uniform conditions.

For a given PV module, in order to evaluate I_{ph}, I_{sat}, η, R_s, R_h in a particular environmental condition, a system of non-linear equations is generated by forcing (1) to fit the I-V curve in five points (**P**1-**P**5):

$$F_{\mathbf{P}i}: \quad I_{ph} - I_{sat}\left(\exp\left(\frac{V_{\mathbf{P}i} + R_s \cdot I_{\mathbf{P}i}}{\eta \cdot V_t}\right) - 1\right) +$$

$$- \frac{V_{\mathbf{P}i} + R_s \cdot I_{\mathbf{P}i}}{R_h} - I_{\mathbf{P}i} = 0 \qquad i \in [1,5] \tag{2}$$

where $I_{\mathbf{P}i}$ and $V_{\mathbf{P}i}$ are the PV current and voltage for the corresponding five-points.

An additional non-linear equation (sixth) is obtained from the derivative of the power in the MPP, as presented in [24]. This equation help to warranty the reproduction of the behavior of the P-V curve in the MPP. Moreover, including this equation it was obtained an improvement in the convergence of the optimization algorithm.

$$F_{\mathbf{P}6}: \quad \frac{\partial P}{\partial V}\Big|_{MPP} = 0 \tag{3}$$

$$F_{\mathbf{P}6}: \quad \frac{-\eta \cdot V_t - I_{sat} \cdot R_h \cdot e^{x_p}}{\eta \cdot V_t \cdot (R_s + R_h + I_{sat} \cdot R_h \cdot R_s \cdot e^{x_p})} + \frac{I_{mpp}}{V_{mpp}} = 0$$

$$x_p = \frac{V_{mpp} + I_{mpp} \cdot R_s}{\eta \cdot V_t}$$

The points ($\mathbf{P}1$ - $\mathbf{P}5$), shown in Fig. 2, have been selected according to [22]; thus, the corresponding values $I_{\mathbf{P}i}$ and $V_{\mathbf{P}i}$ can be estimated by using explicit King's equations provided that the irradiance and temperature conditions are given. Those points can be obtained from an experimental I-V curve, by selecting the values closest to $\mathbf{P}1$ - $\mathbf{P}5$, or from the SAM database. It is worth noting that the irradiance (G) and module temperature (T) are measured, and that the experimental measurement of the I-V curve must be performed as fast as possible (few milliseconds), so that an approximately constant G and T can be assumed.

3. Numerical solution by means of genetic algorithm

The resulting system composed of six non-linear equations cannot be solved easily by using traditional methods like Newton-Raphson since the number of
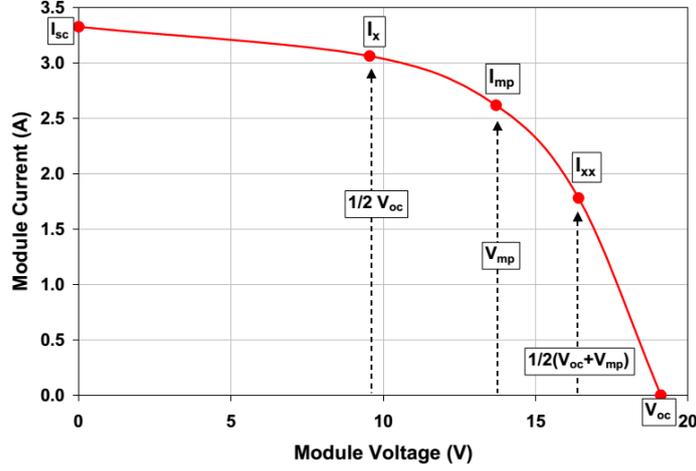
Figure 2: Five key points of an I-V curve proposed in [22].

equations is higher than the number of unknowns. Even eliminating one of the equations to obtain a systems with five equations and five unknowns, the values of the parameters are in different ranges (e.g. I_{ph} is in the order of amperes, while I_{sat} is in the order of nano-amperes) and all the equations are transcendental and non-linear. Therefore, the system to be solved is highly non-linear and ill-conditioned; consequently, suitable methods are needed for its solution [24, 19, 31].

The approach used in this paper is to pose the solution of the non-linear equations system as an optimization problem that considers a combination of the non-linear functions $F_{\mathbf{P}1}$ to $F_{\mathbf{P}6}$ as a cost function (FC) to be minimized:

$$FC(I_{ph}, I_{sat}, \eta, R_s, R_h) = \sum_{i=1}^{6} F_{\mathbf{P}i}^2 \qquad (4)$$

3.1. Genetic algorithm

The Genetic Algorithm (GA) is a technique for solving constrained and unconstrained optimization problems inspired to the biological evolution. In GA each individual represents a solution, whereby, in the parameter estimation

7

problem, each individual is a set of the single-diode model parameters (i.e. individual i contains $I_{ph,i}$, $I_{sat,i}$, η_i, $R_{s,i}$ and $R_{h,i}$).

The GA starts with a set of individuals created randomly in the search range denominated initial population. To create the new generation the algorithm selects some individuals of the current population as "parents" to contribute part of their genes (in this case the PV module parameters) to create "children". Those children are the individuals of the new generation.

There are three different types of children: Elite, Crossover and Mutation. The individuals of the present generation with the lowest cost function values survive as children of the next generation, those are the Elite children. Other group of children (Crossover) are created by combining the genes or vectors of two parents; therefore, each children has information of the genes of both parents. Finally, the Mutation children are created by modifying the genes of the parents randomly, in other words a Mutation child is created by modifying one parent only.

In general, the GA continues creating new generations until a stop condition is fulfilled. Some typical stopping conditions are: desired fitness function range, maximum number of generations, time limit or the relative change in the fitness function.

The genetic algorithm, available in the Global Optimization toolbox of Matlab, has been used for minimizing the cost function (4). The configuration parameters of the GA are summarized in Table 1 and their selection is explained below.

3.2. Selection of the GA parameters

The parameters defined for the GA are presented in Table 1. The population size is selected after an analysis of the performance with different values, from 5 to 100 in steps of 5, for the PV module operating in NOCT conditions ($G = 800\ W/m^2$ and $T = 47\ ^oC$). This procedure enables to find a tradeoff between accuracy (i.e. low fitness values) and computational burden (i.e. number of fitness evaluations). The procedure is repeated 30 times to analyze the average

performance of the GA with different population sizes. The results of such simulations are presented in Fig. 3, where it can be observed that: between 15 and 40 individuals the average fitness values are similar, but the average fitness evaluations (computational burden) increases significantly; therefore, 20 individuals is selected to obtain a tradeoff between a low value of the fitness function with a reasonable computational burden. Moreover, such value has also been used by other authors to solve this problem [4, 39].
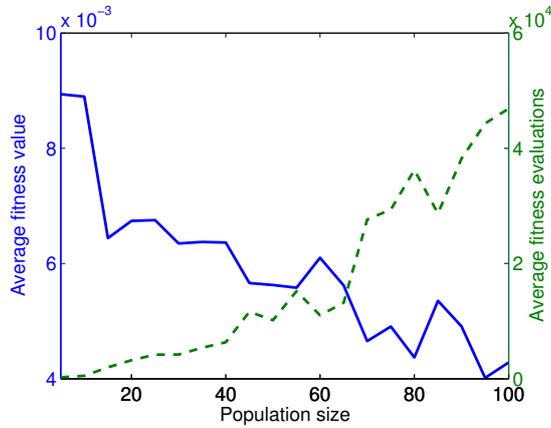
Figure 3: Effects of Population Size parameter on the fitness value and generations number.

In the initial population one or more individuals can be introduced by the user. Such option is used in the proposed method to introduce the analytical solution presented in [1] as one individual of the initial population, this to provide the GA a solution that can be close to the optimal and reduce the convergence time. The other the individuals of the initial population are created using "Feasible population" function which is able to handle the given boundaries for the genes' values.

One important element proposed in this paper is the restriction of the initial population in a feasible range defining the limits described in (13)-(17). This is important because it depends on the guess solution for the given PV module.

Two scaling functions in the Matlab toolbox that can be used for this op-

timization problem were evaluated: "Rank" and "Top". "Rank" function provided the best results (lower fitness and current errors) and it has a random component that helps to maintain the diversity of the individuals. To choose the selection function stochastic uniform, roulette and tournament methods were evaluated and they provided similar performances; however, tournament method provided the lowest errors in the current predictions.

The selection of the Crossover and Mutation functions, "intermediate" and "adaptive feasible", respectively, were selected because they are able to consider constraints and boundaries. Moreover, "intermediate" also has an aleatory component and, unlike other crossover functions, it is able to handle boundaries.

Two important parameters of the GA are Elite count and Crossover fraction. On one hand, Elite count specify how many of the best individuals in the actual generation will survive as children of the next one. On the other hand, Crossover fraction is the percentage of the next generation that will be created by crossover. The rest of the population is created by mutation. To select these parameters a numerical evaluation was performed with the BP858 PV panel at normal operating test conditions ($G = 0.8 \ kW/m^2$ and $T = 47 \ ^oC$) taking the five reference values by using the model proposed in [22]. Different Elite count (from 2 to 18 with steps of 2) values and Crossover fraction (from 0.1 to 0.9 with steps of 0.1) were tested to define their appropriate ranges. The minimum fitness values are presented in Fig. 4 where it can be observed the region of values that provide the lowest cost function. Finally, Elite count and Crossover fraction were selected in the center of the mentioned region (Elite count: 15 and Crossover fraction: 85 %).

3.3. Guess solution and boundaries of the module parameters

The guess solution ($I_{ph,0}$, $I_{sat,0}$, η_0, $R_{s,0}$, $R_{h,0}$) is calculated by using the explicit equations (5), (6), (7), (10) and (11), respectively. Such equations are obtained by performing some approximations on the analytical expression of the PV equation as shown in [1].

10
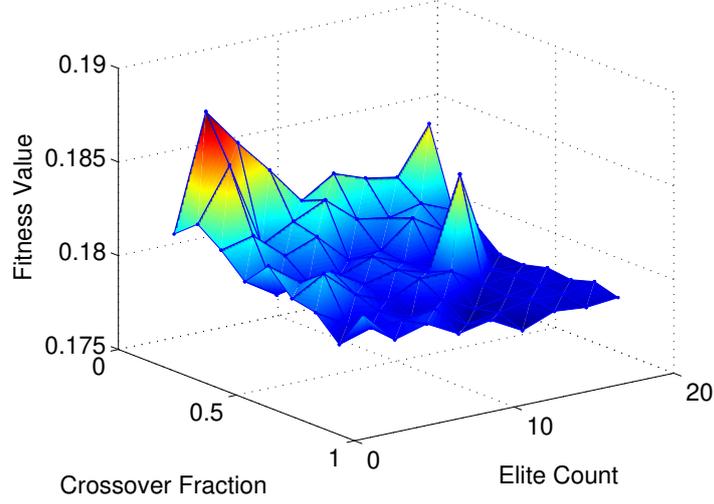
Figure 4: Effects of Elite Count and Crossover Fraction parameters on the fitness value.

$$I_{ph,0} \approx I_{sc} \tag{5}$$

$$I_{sat,0} = I_{ph} \cdot e^{-\frac{V_{oc}}{\eta \cdot V_t}} \tag{6}$$

$$\eta_0 = \frac{\alpha_{Voc} - V_{oc}/T}{V_t \cdot \left(\frac{\alpha_{Isc}}{I_{ph}} - \frac{3}{T} - \frac{E_{gap}}{k \cdot T^2} \right)} \tag{7}$$

$$\Theta = \frac{V_{mpp} \cdot (2 \cdot I_{mpp} - I_{ph}) \cdot e^{\frac{V_{mpp} \cdot (V_{mpp} - 2 \cdot \eta \cdot V_t)}{(\eta \cdot V_t)^2}}}{\eta \cdot V_t \cdot I_{sat}} \tag{8}$$

$$x = W[\Theta] + 2 \cdot \frac{V_{mpp}}{\eta \cdot V_t} - \frac{V_{mpp}^2}{(\eta \cdot V_t)^2} \tag{9}$$

$$R_{s,0} = \frac{x \cdot \eta \cdot V_t - V_{mpp}}{I_{mpp}} \tag{10}$$

$$R_{h,0} = \frac{x \cdot \eta \cdot V_t}{I_{ph} - I_{mpp} - I_{sat} \cdot (e^x - 1)} \tag{11}$$

In those equations: α_{Voc} and α_{Isc} are the temperature coefficients of the open-circuit voltage (V_{oc}) and short-circuit current (I_{sc}), respectively, and E_{gap} is the energy gap of the semiconductor. $W[\cdot]$ is the Lambert-W function representing the solution of the equation $\Theta = x \cdot e^x$.

Table 1: Genetic Algorithm settings

Parameter	Set value(s)
Population type	Double vector
Population size	20
Initial Population	Result of equations (5)-(7), (10) and (11)
Creation function	Feasible population
Initial range	See (13)-(17)
Scaling function	Rank
Selection function	Tournament
Elite count	15
Crossover fraction	85 %
Crossover	Intermediate
Mutation function	Adaptive Feasible
Lower bound	$I_{ph} = I_{sc}$, $I_{sat} = 1 \cdot 10^{-10}$ A, $\eta = 0.5$, $R_s = 0.01$ Ω, $R_h = 10$ Ω
Upper bound	$I_{ph} = 1.5 \cdot I_{sc}$, $I_{sat} = 1 \cdot 10^{-2}$ A, $\eta = 5$, $R_s = 10$ Ω, $R_h = 10$ $k\Omega$

The lower and upper bounds (see Table 1) and the initial population ranges ((13)-(17)) defined for the five parameters (I_{ph}, I_{sat}, η, R_s and R_h) have been derived on the basis of physical constraints on the electrical circuit of Fig. 1 as well as references found in literature [12, 15, 11, 35] about the variations of those parameters.

The ideality factor (η) lumps the effect of the two ideality factors of the double diode model [12]. Ideally η assumes a value of one [15]; however, the different semiconductor materials and degradation effects make the η value as high as two [15] or even four in some cases. From that information, the initial population range of η was selected with respect to η_0 plus/minus one (14). The upper and lower bounds of η in the GA have been defined as 0.5 and 5 (see Table 1), respectively, to provide a range wide enough to cover different materials and

degradation effects.

According to [15] the values of the inverse saturation current in a PV cell are around 10^{-10} to 10^{-6} A/cm^2. A typical cell has an area of hundreds of cm^2, thus a feasible range for I_{sat} is the orders 10^{-8} to 10^{-4} A. Such variation of four orders of magnitude was considered to selected the initial population range with respect to $I_{sat,0}$ as shown in (15). The upper and lower bounds has been selected as 10^{-10} and 10^{-2}.

Typically series resistance take values of hundreds of $m\Omega$ [12, 35]; however, due to degradation effects it can be increased up to ten times its initial value [11, 35]. Hence, on one hand, the initial range has been defined as one-tenth to ten times it initial value ($R_{s,0}$) as shown in (16). On the other hand, the upper ($R_{s,ub}$) and lower ($R_{s,lb}$) bounds has been defined as 0.01 Ω and 10.0 Ω to include the possible values of R_s for different modules. For R_h the values reported in literature vary from tens of Ohms [35] to hundreds [36] or even thousands [26] of Ohms. Taking into account that the variations are in two orders of magnitude, the initial population range has been defined as 0.1 and 10 times $R_{h,0}$ (17) and the search range goes from 10 Ω ($R_{h,lb}$) to 10 $k\Omega$ ($R_{h,ub}$).

In the case of I_{ph}, it must be equal or higher than the short-circuit current (I_{sc}). Evaluating (1) in the short-circuit point and neglecting the diode current (since I_{sc} in amperes and diode current in μA or nA) it can be defined the upper limit of the initial population range of I_{ph} ($I_{ph,ul}$) as (12). Meanwhile, the search range has been restricted from I_{sc} to $1.5 \cdot I_{sc}$, since even in the worst-case scenario the difference between I_{ph} and I_{sc} would be less than 50 %.

$$I_{ph,ul} = I_{sc} \cdot \left(1 + \frac{R_{s,0}}{R_{h,0}}\right) \tag{12}$$

$$I_{sc} < I_{ph} < I_{ph,ul} \tag{13}$$

$$\eta_0 - 1 < \eta < \eta_0 + 1 \tag{14}$$

$$10^{-2} \cdot I_{sat,0} < I_{sat} < 10^2 \cdot I_{sat,0} \tag{15}$$

$$0.1 \cdot R_{s,0} < R_s < 10 \cdot R_{s,0} \tag{16}$$

$$0.1 \cdot R_{h,0} < R_h < 10 \cdot R_{h,0} \tag{17}$$

3.4. Impact of the parameter errors

This section shows the effects in the reproductions of the characteristic curves of a PV module produced by the errors in the five parameters of the single diode model. Such an analysis allows the identification of the parameters (I_{ph} and η) that more affect reconstruction of the characteristic curves by using the single diode model.

The errors in the module current (I) induced by errors in the parameters, considering (1), are given in (18)-(22). In such expressions where ΔI represents the error on I and ΔI_{ph}, ΔI_{sat}, $\Delta \eta$, ΔR_s and ΔR_h represent the errors in the parameters.

$$\Delta I = \frac{\partial I}{\partial I_{ph}} \Delta I_{ph} \quad , \quad \frac{\partial I}{\partial I_{ph}} = 1 \tag{18}$$

$$\Delta I = \frac{\partial I}{\partial I_{sat}} \Delta I_{sat} \quad , \quad \frac{\partial I}{\partial I_{sat}} = 1 - \exp\left(\frac{V + I \cdot Rs}{V_t \cdot \eta}\right) \tag{19}$$

$$\Delta I = \frac{\partial I}{\partial \eta} \Delta \eta \quad , \quad \frac{\partial I}{\partial \eta} = I_{sat} \cdot \exp\left(\frac{V + I \cdot R_s}{V_t \cdot \eta}\right) \cdot \left(\frac{V + I \cdot R_s}{V_t \cdot \eta^2}\right) \tag{20}$$

$$\Delta I = \frac{\partial I}{\partial R_s} \Delta R_s \quad , \quad \frac{\partial I}{\partial R_s} = -\frac{I}{R_h} - \frac{I \cdot I_{sat} \cdot \exp\left(\frac{V + I \cdot R_s}{V_t \cdot \eta}\right)}{V_t \cdot \eta} \tag{21}$$

$$\Delta I = \frac{\partial I}{\partial R_h} \Delta R_h \quad , \quad \frac{\partial I}{\partial R_h} = \frac{V + I \cdot R_s}{R_h^2} \tag{22}$$

Without loss of generality, such relations will be illustrated using monocrystalline silicon panel (BP585), whose nominal parameters are extracted from the electrical information in the manufacturer datasheet by using (5)-(11): $I_{ph} = 5.0\ A$, $I_{sat} = 2.8088 \times 10^{-9}\ A$, $\eta = 1.1218$, $R_s = 0.2275\ \Omega$ and $R_h = 2.0290\ k\Omega$.

From (18) it can be noted that the errors in I_{ph} directly affect the value of the module current, which can be confirmed by observing (1), since I_{ph} is a term in the same range of I. Partial derivatives of I, with respect to I_{sat} (19) and η (20), have negative and positive exponential terms, respectively, which assume low magnitudes at low and middle voltages, and high magnitudes at high voltages. However, on one hand, percentual errors I_{sat} modify the inverse saturation currents in few micro-amperes; therefore, it is expected that errors in this parameter do not considerably affect I. On the other hand, errors in η considerably affect I, since η is inside the two exponential multiplicands in (20): as η in one of them, and as η^2 in the other.

Evaluating (21) it can be observed that it presents low magnitudes for low and middle voltages, but considerable magnitudes for high voltages. Thus, considering the low magnitude of R_s, the errors induced by this parameter are low. Finally, observing (22) it can be noted that R_h^2 is dividing all the terms; taking into account the large magnitude of R_h with respect to $V + I \cdot Rs$, it can be deduced that errors induced by that parameter are not representative in the calculation of I.

Fig. 5 shows the errors introduced in I by $\pm 10\%$ errors on the model parameters. As predicted in the previous paragraph, errors on I_{sat}, R_s and R_h have less impact on the module current calculation than errors on both I_{ph} and η. Thus, the current and voltage prediction of a PV module are mainly affected by errors on I_{ph} and η, respectively. Therefore, due to the small sensitivity of I to changes on I_{sat}, R_s and R_h in comparison with changes on I_{ph} and η, larger estimation errors on I_{sat}, R_s and R_h are expected in comparison with the estimation errors on η and I_{sc}.

4. Performance of the genetic algorithm

A mono-crystalline silicon panel (BP585) with 36 cells ($N_s = 36$) was selected as an example to illustrate the application of the method and the variation of the parameters for different irradiance and temperature conditions. The main

electrical characteristics of the selected panel in STC (irradiance of 1 kW/m^2 and cells temperature of 25 ^{o}C) are listed in Table 2.

Table 2: Datasheet Parameters of BP585 (2002)

Parameter (STC)	Value
Open Circuit Voltage ($V_{oc,STC}$)	22.1 V
Short Circuit Current ($I_{sc,STC}$)	5.00 A
MPP Voltage ($V_{mpp,STC}$)	18.0 V
MPP Current ($I_{mpp,STC}$)	4.70 A
Voc Temperature Constant (α_{Voc})	-0.088 V/ ^{o}C
Isc Temperature Constant (α_{Isc})	0.047 %/ ^{o}C
Number of Cells (N_s)	36

For the PV panel under test the points **P**1 to **P**5 were calculated by using the King's equations proposed in [22] and the coefficients provided by SAM database.

Fig. 6 and Fig. 7 show the matching between the I-V curves reproduced with the single-diode model, whose parameters have been estimated with the GA, and the reference points calculated with the King's equations for the environmental conditions reported in Table 3 and Table 4.

Table 3: Estimated parameters @ $T = 25^o$**C**

G [**W/m**^{2}]	**1000**	**600**	**200**
I_{ph} [**A**]	5.000	3.000	1.000
I_{sat} [**nA**]	2.808	2.397	1.957
η	1.121	1.111	1.092
R_s [Ω]	0.227	0.282	0.500
R_h [$k\Omega$]	2.029	1.914	5.858

Table 4: Estimated parameters @ $G = 1000$ **W/m^2**

T [^oC]	**35**	**45**	**55**
I_{ph} [**A**]	5.023	5.047	5.070
I_{sat} [**nA**]	12.30	49.32	182.26
η	1.119	1.117	1.115
R_s [Ω]	0.226	0.224	0.249
R_h [$k\Omega$]	1.317	1.112	1.162

4.1. Evolution analysis

The proposed method was applied 20 times to extract the parameters of a BP585 panel, considering an irradiance of 800 W/m^2 and temperature of 47 ^oC, in order to analyze the evolution of the best individual of the population and the module parameters.

The evolution of the parameters for the 20 trials is presented in Fig. 8. The dotted lines represent the guess values of the parameters calculated following the equations presented in Section 3.3. In general, the parameters provided by the guess solution are close to the final values obtained with the optimization procedure, which shows that the guess solution is important to reduce the convergence time of the GA. Additionally, Fig. 8 evidence that: the GA finds a solution different but close to the guess solution, and the parameters obtained in the 20 trials are close among them. These points evidence the consistency of the solutions offered by the proposed method.

Fig. 9(a) shows the maximum, minimum and average values of the fitness function of the best individuals in each generation. The average of best fitness values at the end of the optimization procedure is 0.07834 and the maximum and minimum values are +1.4 % and -3.5 %, respectively, with respect to the average value. The results show that the proposed method arrives to a similar solution in all the cases. It can be observed that the proposed method starts with a fitness value in the same range of the final value (close to 0.08), which helps to reduce the convergence time. Moreover, the standard deviation of the

best individuals in each generation for the 20 trials (Fig. 9(b)) shows that similar results are obtained in all the trials.

4.2. Error analysis

The cost function (4) was minimized, by using "Quasi-Newton" (QN) and "Trust-Region" (TR) algorithms as well as the proposed method (PM), to estimate the parameters the BP585 panel. This procedure is aimed at comparing the errors of the three methods in the reproduction of the five key points of I-V curves for different irradiance and temperature conditions.

QN and TR algorithms require a guess solution to start the minimization of the cost function. In this analysis the guess solution presented in Section 3.3 was used for QN and TR methods, since QN and TR may provide wrong parameters if the guess solution is not close to the solution.

The PV module parameters were estimated for 12 different operating conditions using the three methods (QN, TR and PM). Using those parameters, the five key points of the I-V curves for each operating condition were reconstructed to assess the Normalized Sum of Squared Errors (NSSE) of each method. The NSSE is defined in (23), where y and y_e represent the reference and estimated values, and H represents the number of data.

$$NSSE[\%] = \frac{\sum_{k=1}^{H}(y(k) - y_e(k))^2}{\sum_{k=1}^{H}(y(k))^2} \qquad (23)$$

The NSSE values obtained with the three methods are presented in Table 5 where the columns and rows represent the different irradiances and temperature conditions, respectively, and each cell contains the errors or the three methods marked as PM (Proposed Method), QN (Quasi-Newton) and TR (Trust-Region). The errors obtained with the proposed method are lower than the ones obtained QN and close to the errors obtained with TR algorithms for the different operating conditions; however, the magnitudes of the three methods are similar. It is important to note that, unlike QN and TR algorithms, the low errors obtained with the proposed method can be also obtained without

18

using the initial guess solution; however, in such a case it would be required to increase considerably the population size (e.g. 100), which would increment many times the calculation time. Moreover, increasing the population size it is possible to reduce errors with the proposed method, if it is required; however, it would produce a significant increase in the calculation burden (see Fig. 3).

Table 5: NSS values of the three methods (PM: proposed method, QN: Quasi-Newton and TR: Trust-Region) for different operating conditions

Tempe-rature [^oC]	Method	Irradiance [kW/m^2]			
		1	0.7	0.4	0.1
25	PM	2.285e-3	5.902e-3	1.423e-2	3.845e-2
	QN	2.276e-3	7.462e-3	1.733e-2	4.398e-2
	TR	1.804e-3	5.775e-3	1.345e-2	3.872e-2
45	PM	5.343e-3	1.534e-2	2.964e-2	1.056e-1
	QN	7.485e-3	2.136e-2	3.937e-2	2.233e-1
	TR	1.211e-3	2.144e-3	3.617e-3	9.473e-2
65	PM	1.692e-2	3.642e-2	1.458e-2	2.595e-1
	QN	2.705e-2	5.174e-2	8.164e-2	3.568e-1
	TR	2.541e-3	4.645e-3	6.641e-3	3.514e-3

5. Parameters variations with different irradiance and temperature conditions

This Section shows an application of the proposed parameter estimation method to illustrate the parameters variability with irradiance and temperature. A total of 25 combinations of irradiance and temperature values have been used. Fig. 10 to Fig. 12 show the parameters values trend for the irradiance going from 0.2 to 1 kW/m^2 and for the cell temperature going from 20 to 60 ^{o}C.

This application example is performed because some papers found in literature assume that only I_{ph} and I_{sat} are affected by irradiance and temperature variations, while η, R_s and R_h are constant [36, 24, 11, 27]. However, η, R_s and

R_h can be affected by the environmental conditions and the module degradation. Such relations are not clearly documented in the literature but may affect the accuracy of a PV panel model [19, 10, 26, 2, 33, 37, 21], which may be propagated in the prediction of a PV array current, power and energy production.

The parameters obtained with the proposed method are compared with the traditional equations to calculate the variation of the parameters with respect to irradiance and temperature, which are introduced in equations (24) to (29) [10].

$$I_{ph} = \frac{G}{G_{STC}} \left(I_{ph,STC} + \alpha_{Isc} \left(T - T_{STC} \right) \right) \tag{24}$$

$$E_{gap} = E_{gap,STC} \cdot \left(1 - 0.0002677 \cdot \left(T - T_{STC} \right) \right) \tag{25}$$

$$I_{sat} = I_{sat,STC} \cdot \left(\frac{T}{T_{STC}} \right)^3 \cdot e^{\left(\frac{E_{gap}}{k \cdot T_{STC}} - \frac{E_{gap}}{k \cdot T} \right)} \tag{26}$$

$$\eta = \eta_{STC} \cdot \frac{T}{T_{STC}} \tag{27}$$

$$R_s = R_{STC} \tag{28}$$

$$R_h = R_{h,STC} \cdot \frac{G}{G_{STC}} \tag{29}$$

In Fig. 10 to Fig. 12 the x-axis and y-axis represent the temperature and the parameter value, respectively. The parameters estimated with the proposed procedures are represented by solid lines and the values calculated with equations (24)-(29) are represented by circles. The behavior of the parameters with respect to the irradiance are represented with lines (proposed method) and circle (equations) of different colors.

I_{ph} is the only parameter that matches with the values calculated with (24) (see Fig. 10). It can be observed that I_{ph} is proportional to the irradiance and has a small variations with respect to the temperature.

The traditional equations to adjust the parameters I_{sat} and η only consider temperature variations; however, Fig. 11 shows that I_{sat} and η also vary with respect to the irradiance. Therefore, the irradiance needs to be considered to adjust I_{sat} and η if high accuracy in the reproduction of the I-V curves is

required.

Fig. 11 shows two different points. On one hand, the variations of I_{sat} with the irradiance [24, 17] are small with respect to the values predicted by (26) (see Fig. 11(a)). On the other hand, Fig. 11(a) shows that η has a low sensitivity with the irradiance and a very low sensitivity with the temperature, which contrast with the behavior predicted by (27).

The simulation results show significant differences between the resistances values estimated with the proposed method and the ones predicted by (28) and (29). Fig. 12(a) shows that R_s varies, principally, with the irradiance but also with the temperature. It can be observed that for low irradiances and high temperature values R_s increases many times its nominal value. According to Fig. 12(b) the relation between R_h and the irradiance is not linear as predicted by (29), and R_h is also affected by the temperature. Considering the behavior of R_s and R_h (Fig. 12) it can be deduced that the translation equations, or procedures, of those parameters need to include the operating conditions (i.e. irradiance and temperature).

Finally, the I-V curve for each operating condition was calculated using the parameters obtained with the proposed method and the equations (24)-(29). The NSSE, calculated for the five key points of each I-V curve predicted by the model and the ones obtained by following King's procedure, are shown in Fig. 13. It can be observed that the errors of the proposed model are one order of magnitude smaller the errors using the equations (24)-(29). Additionally, it can be observed that the errors increase at low irradiance and high temperature. Therefore, it is important to consider the variations of the single diode model parameters with respect to the irradiance and temperature to obtain high accuracy in the reproductions of the I-V and P-V curves.

6. Conclusions

A method to calculate the five parameters of the single-diode model of a PV module has been presented. The main objective of the method is to obtain

the values of parameter for any environmental condition without performing any simplification. A system of six non-linear equations, including the power derivative condition in the MPP, is formalized as an optimization problem which is solved through a Genetic Algorithm.

The low NSSE errors obtained in all the curves show the agreement between the predicted I-V curve and the reference points obtained from the King's model [22] and the coefficients in SAM database.

Unlike other works reported in literature where the parameters η, R_s and R_h are considered constant for all irradiance and temperature conditions, in this document has been highlighted that all the parameters change. In particular has been shown that η, R_s and R_h present significant variations according to the weather conditions. The graph of R_h shows that its magnitude is strongly non-linear with respect to the irradiance and temperature variations.

Moreover, due to soiling, aging, degradation, etc., the values of the parameters in the PV model can assume unpredicted drift, thus the proposed approach can be used as a reference for diagnostic purposes because of its capability to use only five operating points for identifying accurately all parameters of the single-diode model.

References

[1] J. Accarino, G. Petrone, C. A. Ramos-Paja, G. Spagnuolo, Symbolic algebra for the calculation of the series and parallel resistances in PV module model, in: 2013 International Conference on Clean Electrical Power (IC-CEP), 2013, pp. 62–66.

[2] F. Adamo, F. Attivissimo, A. di Nisio, M. Spadavecchia, Characterization and testing of a tool for photovoltaic panel modeling, IEEE Trans. on Instrum. and Meas. 60 (5) (2011) 1613–1622.

[3] M. F. AlHajri, K. M. El-Naggar, M. R. AlRashidi, A. K. Al-Othman, Optimal extraction of solar cell parameters using pattern search, Renew. Energy 44 (2012) 238–245.

[4] J. Appelbaum, A. Peled, Parameters extraction of solar cells - a comparative examination of three methods, Sol. Energy Mater. and Sol. Cells 122 (2014) 164–173.

[5] A. Askarzadeh, A. Rezazadeh, Parameter identification for solar cell models using harmony search-based algorithms, Sol. Energy 86 (11) (2012) 3241–3249.

[6] A. Askarzadeh, A. Rezazadeh, Artificial bee swarm optimization algorithm for parameters identification of solar cell models, Appl. Energy 102 (2013) 943–949.

[7] A. S. Bouhouras, A. G. Marinopoulos, D. P. Labridis, P. S. Dokopoulos, Installation of PV systems in Greece-reliability improvement in the transmission and distribution system, Electr. Power Syst. Res. 80 (5) (2010) 547–555.

[8] D. S. H. Chan, J. C. H. Phang, Analytical methods for the extraction of solar-cell single- and double-diode model parameters from I-V characteristics, IEEE Trans. on Electron Devices 34 (2) (1987) 286–293.

[9] A. Chatterjee, Identification of photovoltaic source models, IEEE Trans. on Energy Convers. 26 (3) (2011) 883–889.

[10] W. De Soto, S. Klein, W. Beckman, Improvement and validation of a model for photovoltaic array performance, Sol. Energy 80 (1) (2006) 78–88.

[11] J. Del Cueto, Method for analyzing series resistance and diode quality factors from field data of photovoltaic modules, Sol. Energy Mater. and Sol. Cells 55 (3) (1998) 291–297.

[12] U. Eicker, Solar Technologies for Buildings, John Wiley & Sons, Ltd, Chichester, 2003.

[13] W. Gong, Z. Cai, Parameter extraction of solar cell models using repaired adaptive differential evolution, Sol. Energy 94 (2013) 209–220.

[14] P. Hacke, R. Smith, K. Terwilliger, S. Glick, D. Jordan, S. Johnston, M. Kempe, S. Kurtz, Testing and analysis for lifetime prediction of crystalline silicon PV modules undergoing degradation by system voltage stress, IEEE J. of Photovolt. 3 (1) (2013) 246–253.

[15] H. J. Hovel, Semiconductors and Semimetals: Volume 11 - Solar Cells, Academic Press, New York, 1975.

[16] K. Ishaque, Z. Salam, S. Mekhilef, A. Shamsudin, Parameter extraction of solar photovoltaic modules using penalty-based differential evolution, Appl. Energy 99 (2012) 297–308.

[17] M. S. Ismail, M. Moghavvemi, T. M. I. Mahlia, Characterization of PV panel and global optimization of its model parameters using genetic algorithm, Energy Convers. and Manag. 73 (2013) 10–25.

[18] S. Kaplanis, E. Kaplani, Energy performance and degradation over 20 years performance of BP c-Si PV modules, Simul. Model. Pract. and Theory 19 (4) (2011) 1201–1211.

24

[19] E. Karatepe, M. Boztepe, M. Colak, Neural network based solar cell model, Energy Convers. and Manag. 47 (9-10) (2006) 1159–1178.

[20] K. Kato, "PVRessQ!" PV module failures observed in the field, in: Photovoltaic Module Reliability Workshop 2012, 2012, pp. 1–24.

[21] W. Kim, W. Choi, A novel parameter extraction method for the one-diode solar cell model, Sol. Energy 84 (6) (2010) 1008–1019.

[22] D. L. King, W. E. Boyson, J. A. Kratochvill, Photovoltaic array performance model, Tech. rep., Sandia National Laboratories, Albuquerque (Dec. 2004).

[23] X. Lingyun, S. Lefei, H. Wei, J. Cong, Solar cells parameter extraction using a hybrid genetic algorithm, in: 2011 Third International Conference on Measuring Technology and Mechatronics Automation, 2011, pp. 306–309.

[24] V. Lo Brano, G. Ciulla, An efficient analytical approach for obtaining a five parameters model of photovoltaic modules using only reference data, Appl. Energy 111 (2013) 894–903.

[25] E. L. Meyer, E. E. van Dyk, Assessing the reliability and degradation of photovoltaic module performance parameters, IEEE Trans. on Reliab. 53 (1) (2004) 83–92.

[26] A. Orioli, A. Di Gangi, A procedure to calculate the five-parameter model of crystalline silicon photovoltaic modules on the basis of the tabular performance data, Appl. Energy 102 (2013) 1160–1177.

[27] H. Patel, V. Agarwal, MATLAB-based modeling to study the effects of partial shading on PV array characteristics, IEEE Trans. on Energy Convers. 23 (1) (2008) 302–310.

[28] H. Qin, J. W. Kimball, Parameter determination of photovoltaic cells from field testing data using particle swarm optimization, in: 2011 IEEE Power and Energy Conference at Illinois (PECI), 2011, pp. 4–7.

25

[29] N. Rajasekar, N. Krishna Kumar, R. Venugopalan, Bacterial foraging algorithm based solar PV parameter estimation, Sol. Energy 97 (2013) 255–265.

[30] D. Sera, R. Teodorescu, P. Rodriguez, PV panel model based on datasheet values, in: 2007 IEEE International Symposium on Industrial Electronics, 2007, pp. 2392–2396.

[31] M. U. Siddiqui, M. Abido, Parameter estimation for five- and seven-parameter photovoltaic electrical models using evolutionary algorithms, Appl. Soft Comput. 13 (12) (2013) 4608–4621.

[32] M. U. Siddiqui, A. F. M. Arif, A. M. Bilton, S. Dubowsky, M. Elshafei, An improved electric circuit model for photovoltaic modules based on sensitivity analysis, Sol. Energy 90 (2013) 29–42.

[33] J. J. Soon, K. S. Low, Photovoltaic model identification using particle swarm optimization with inverse barrier constraint, IEEE Trans. on Power Electron. 27 (9) (2012) 3975–3983.

[34] B. Sopori, P. Basnyat, S. Devayajanam, S. Shet, V. Mehta, J. Binns, J. Appel, Understanding light-induced degradation of c-Si solar cells, in: 2012 38th IEEE Photovoltaic Specialists Conference (PVSC), 2012, pp. 1115–1120.

[35] E. van Dyk, E. Meyer, Analysis of the effect of parasitic resistances on the performance of photovoltaic modules, Renew. Energy 29 (3) (2004) 333–344.

[36] M. G. Villalva, J. R. Gazoli, E. R. Filho, Comprehensive approach to modeling and simulation of photovoltaic arrays, IEEE Trans. on Power Electron. 24 (5) (2009) 1198–1208.

[37] G. H. Yordanov, O. M. Midtgard, T. O. Saetre, Two-diode model revisited: parameters extraction from semi-log plots of I-V data, in: 25th European Photovoltaic Solar Energy Conference and Exhibition / 5th World Conference on Photovoltaic Energy Conversion, 2010, pp. 6–10.

[38] X. Yuan, Y. Xiang, Y. He, Parameter extraction of solar cell models using mutative-scale parallel chaos optimization algorithm, Sol. Energy 108 (2014) 238–251.

[39] M. Zagrouba, A. Sellami, M. Bouaïcha, M. Ksouri, Identification of PV solar cells and modules parameters using the genetic algorithms: application to maximum power extraction, Sol. Energy 84 (5) (2010) 860–866.
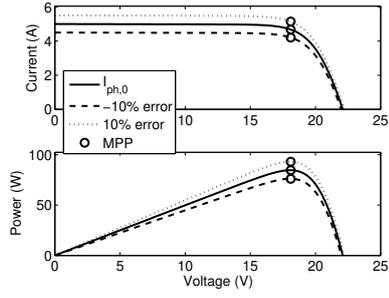
(a) Errors induced by ΔI_{ph}.
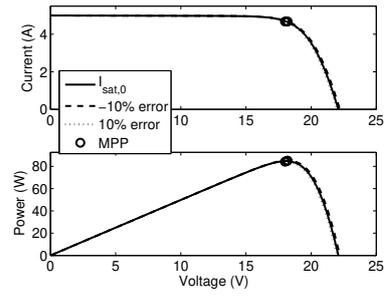
(b) Errors induced by ΔI_{sat}.
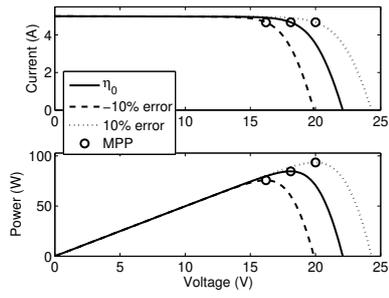
(c) Errors induced by $\Delta\eta$.
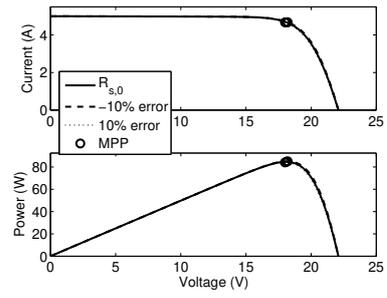
(d) Errors induced by ΔR_s.
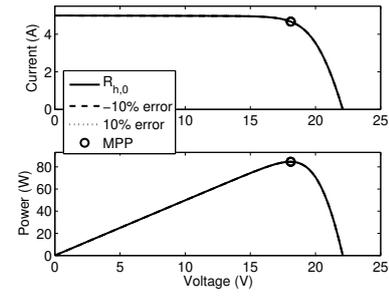
(e) Errors induced by ΔR_h.

Figure 5: Errors in I induced by errors in the parameters.
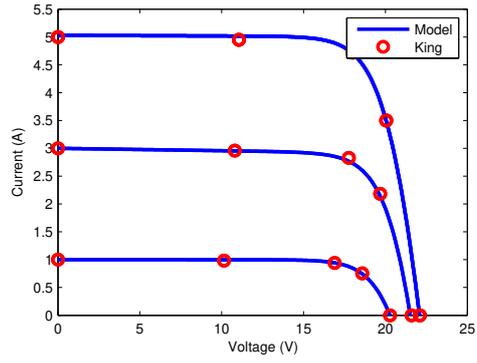
Figure 6: I-V curves obtained with the calculated parameters for different irradiances.
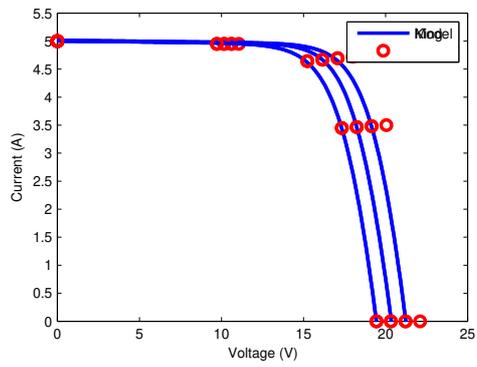
Figure 7: I-V curves obtained with the calculated parameters for different temperatures.

(a) Evolution of I_{ph}.

(b) Evolution of I_{sat}.

(c) Evolution of η.

(d) Evolution of R_s.
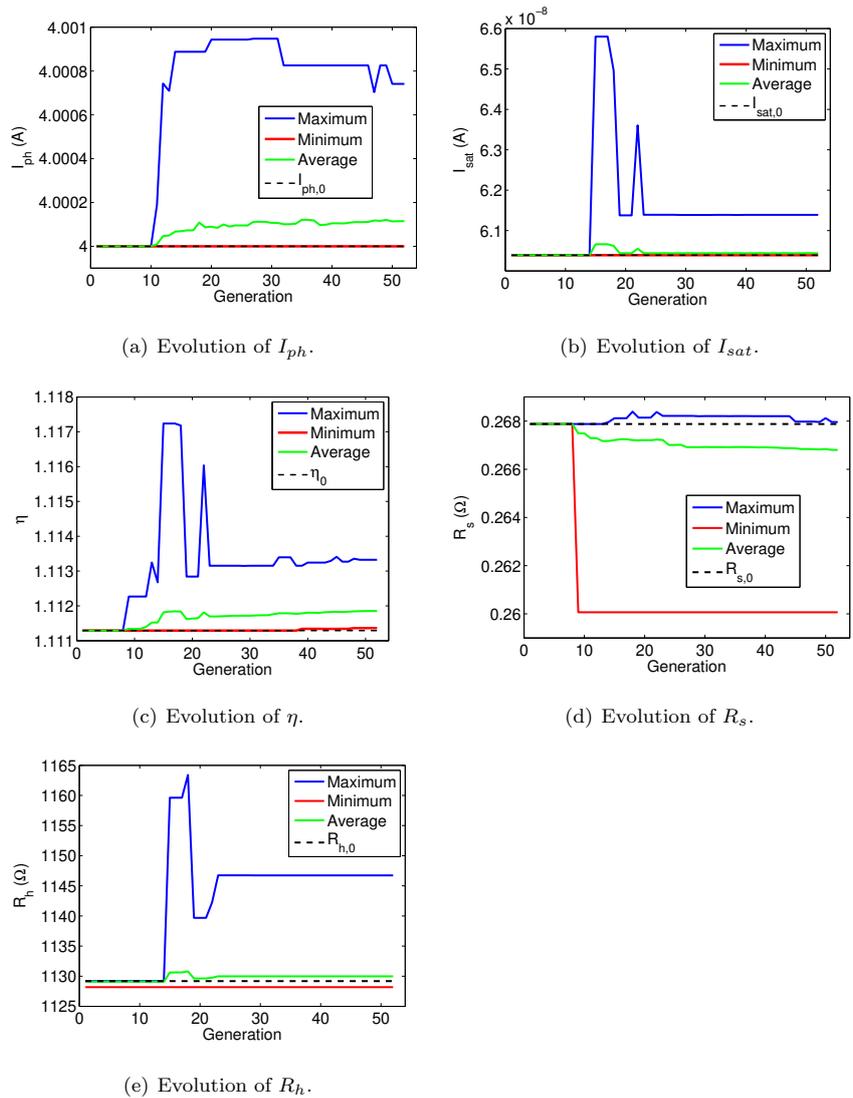
(e) Evolution of R_h.

Figure 8: Evolution of the parameters for 20 trials of the proposed method.
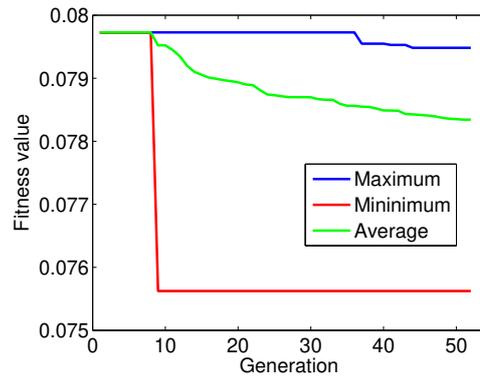
(a) Best fitness value in each generation.
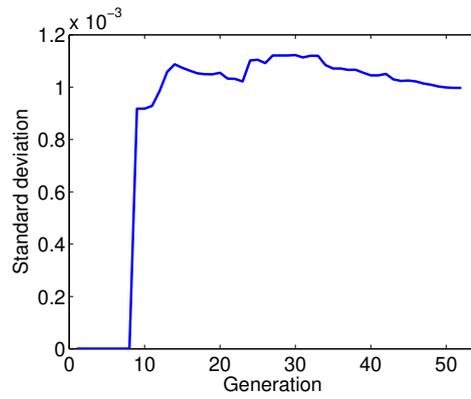
(b) Standard deviation of best fitness values in each generation.

Figure 9: Evolution of the best individual for 20 trials of the proposed method.

31
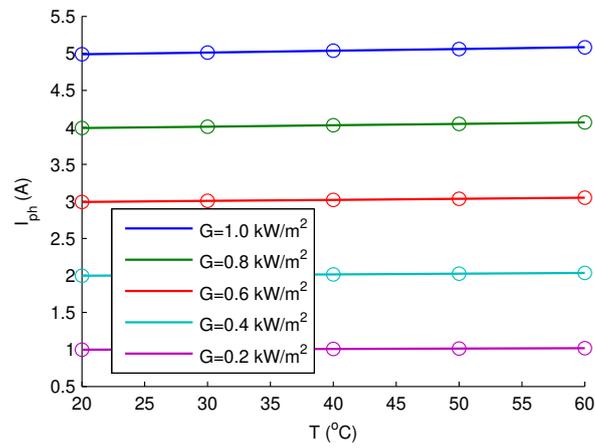
Figure 10: I_{ph} for different irradiance and temperature conditions. Lines: parameter calculated by using the proposed method, circles: parameters calculated by using traditional equations. Each color (lines and circles) represents a different irradiance.
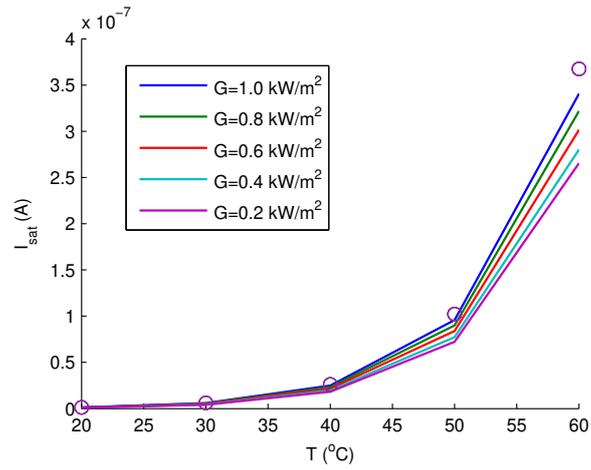
(a) I_{sat} for different irradiance and temperature conditions.
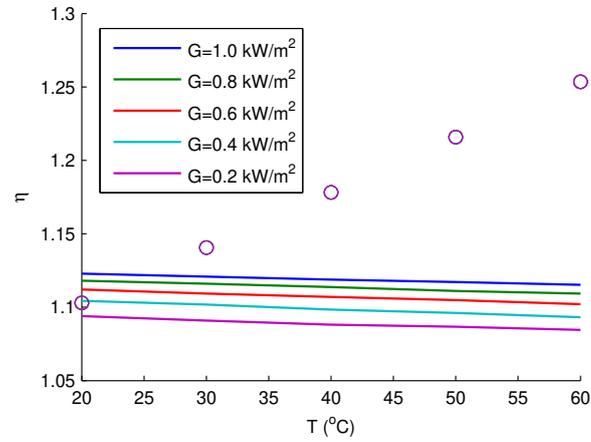
(b) η for different irradiance and temperature conditions.

Figure 11: Parameters values for different irradiance and temperature conditions. Lines: parameters calculated by using the proposed method, circles: parameters calculated by using traditional equations. Each color (lines and circles) represents a different irradiance.
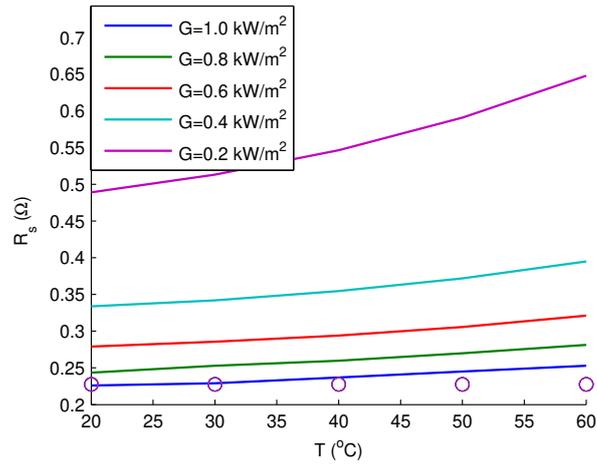
(a) R_s for different irradiance and temperature conditions.
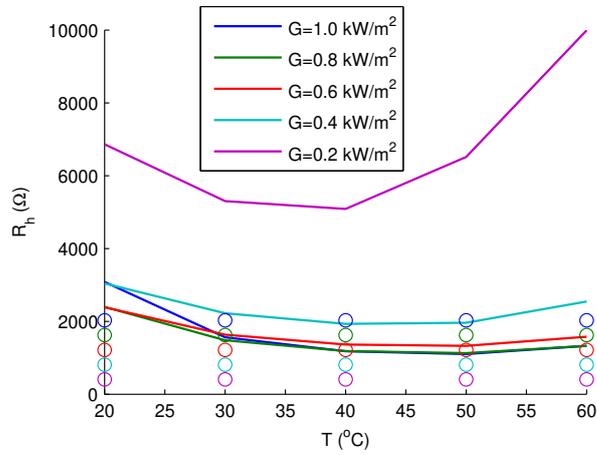

(b) R_h for different irradiance and temperature conditions.

Figure 12: Parameters values for different irradiance and temperature conditions. Lines: parameters calculated by using the proposed method, circles: parameters calculated by using traditional equations. Each color (lines and circles) represents a different irradiance.
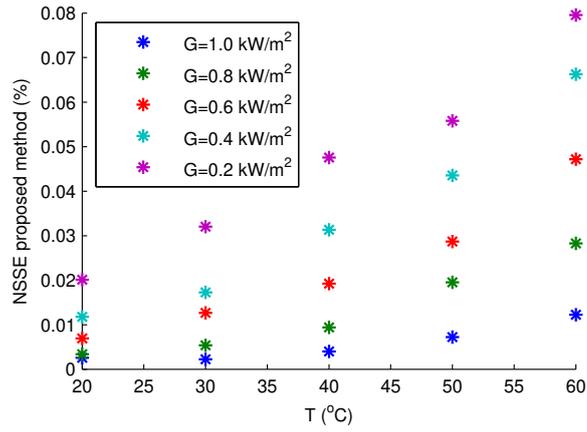
(a) Proposed method.
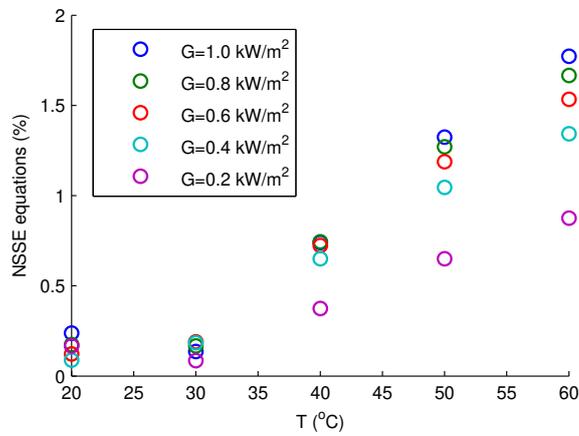
(b) Traditional equations

Figure 13: *NSSE* for the I-V curve in different irradiance and temperature conditions. Stars: error obtained by using the proposed method, circles: errors obtained by using traditional equations. Each color represents a different irradiance.